Environmental Sciences Europe

RESEARCH

Open Access

Multiple physiological response analyses aid the understanding of sensitivity variation between *Microcystis aeruginosa* and *Chlorella* sp. under paraquat exposures

Fang Bai[1,2], Yunlu Jia[1*], Cuiping Yang[1,3], Tianli Li[1], Zhongxing Wu[4], Jin Liu[1] and Lirong Song[1*]

Abstract

Background: Sensitivity differences to chemical pollutants in different phytoplankton species may potentially shape the community structure of phytoplankton. However, detailed information supporting the understanding of sensitivity variations between phytoplankton species is still limited.

Results: To investigate sensitivity differences between the cyanobacterium *Microcystis aeruginosa*, and the green alga *Chlorella* sp. to paraquat, multiple physiological parameters were measured and compared through acute and chronic toxicity assays. Early photosynthetic responses during acute toxicity assays showed that paraquat affects Photosynthesis System II energy fluxes in *M. aeruginosa* within 3 h of exposure, but not in *Chlorella* sp. After 5 h of cumulative exposure, an EC_{50} based on the maximum quantum yield for primary photochemistry of 0.54 mg L^{-1} was achieved and remained more or less constant, while the EC_{50} values for *Chlorella* fluctuated around 44.76 ± 3.13 mg L^{-1} after 24 h of exposure. During chronic 96 h exposure to paraquat, differences in antioxidant enzyme activities, reactive oxygen species (ROS) levels, and ultrastructure were observed in both *M. aeruginosa* and *Chlorella* sp. An increase in the intracellular levels of ROS and the number of plasma membrane damaged cells was observed in *M. aeruginosa* in the 0.2, 0.5, and 1.0 mg L^{-1} treatments ($p < 0.01$), but not for *Chlorella*. In addition, at an exposure level of 1.0 mg L^{-1}, extensive disruption of cell structure was observed in *M. aeruginosa*. Conversely, little disarrangement of organelle structure was found in *Chlorella* sp.

Conclusion: These results confirm that paraquat is more toxic to *M. aeruginosa* than to *Chlorella* sp. The sensitivity differences between these two species (one a prokaryote and the other a eukaryote) to paraquat might be partially explained by the differences in cell structure (cell wall and photosynthetic structure), the enzymatic antioxidant system, and the physiological vulnerability. The multiple physiological endpoint analysis approach used in the current study provides more detailed information for understanding the mechanisms of sensitivity variation between these phytoplankton species.

Keywords: Early response, Chronic response, Growth inhibition, Photosynthesis-inhibiting herbicide, Phytotoxicity, Phytoplankton community

*Correspondence: jiayunlu@ihb.ac.cn; lrsong@ihb.ac.cn
[1] State Key Laboratory of Freshwater Ecology and Biotechnology, Institute of Hydrobiology, Chinese Academy of Sciences, Wuhan 430072, China
Full list of author information is available at the end of the article

Background

Microalgae play a crucial role as primary producers in the aquatic food web and it is expected that any damage produced by environmental stressors (e.g., chemical pollutants) will likely affect higher trophic levels [1]. The phytoplankton community in a freshwater ecosystem is diverse and often includes cyanobacteria and green microalgae as major components [2]. The sensitivity of different phytoplankton species towards chemical pollutants is highly variable [3–5]. At a community level, chemical pollutants might exert selective pressure on phytoplankton community structure. Thus, understanding the physiological basis of sensitivity variation of different species provides the knowledge to explain the adverse outcome pathways of these chemical pressures at the ecological level.

Meanwhile, ecotoxicological assessment of chemical pollutants on phytoplankton has generally been focused on the growth inhibition as a common endpoint, because this is ecologically relevant [4, 6, 7]. However, several sub-cellular physiological and biochemical processes showed faster or stronger effects than apical growth inhibition in unicellular algae-based assays when exposed to toxicants [8]. For instance, Prado et al. reported that after only 24 h of exposure to 0.05 μM paraquat, significant DNA damage was observed in *Chlamydomonas moewusii* Gerloff, while the growth rate was not affected [9]. Parameters associated with oxidative stress, DNA damage, and cell apoptosis (the mitochondrial membrane potential parameter) have also been shown to be highly sensitive endpoints in unicellular algae exposed to different concentrations of prooxidant pollutants [10, 11]. Moreover, in comparison with single endpoint-based assays (i.e., growth inhibition of phytoplankton), multiple endpoint assays can offer a more comprehensive understanding of the risk presented by toxicants by providing important insights into their modes of action [8]. Chakraborty et al. have evaluated the toxicity of malathion on *Anabaena sphaerica* Bornet and Flahault using the multiple endpoint approach and found that toxicity resulted in oxidative stress within the cell [12]. However, *A. sphaerica* could ameliorate the toxicity through the production of superoxide dismutase (SOD), catalase (CAT), ascorbic acid peroxidase, and antioxidants including phenolics and flavonoids. In addition, multiple physiological endpoint experiments can improve our understanding of the mode of action of herbicides on different phytoplankton species [13]. Thus, in the present study, multiple cellular level endpoints were used to study the relative sensitivity of two different phytoplankton species to the photosynthesis inhibitor—paraquat (1, 1′-dimethyl-4, 4′-bipyridilium dichloride).

Furthermore, xenobiotic chemicals affect algal cells as a result of toxicokinetic and toxicodynamic processes. Chemicals can enter algal cells, and reach equilibrium between internal and external concentrations within minutes, while damage cumulatively increases over a period of hours [14, 15]. In addition, the previous research showed that the toxicological effects of a chemical on phytoplankton differ in acute and chronic tests [16, 17]. Therefore, to gain a better and more comprehensive understanding of the mechanisms underlying the modes of action of toxicants, comparative acute and chronic response experiments should be carried out.

Paraquat—a nonselective herbicide widely used to prevent the growth of weeds and grasses—was selected as the photosynthesis inhibitor "model chemical" in this study. It has been known to exert its toxic effects by catalyzing the transfer of electrons from photosystem I (PS I) within the thylakoid membrane, to molecular oxygen by producing oxygen radicals that cause lipid peroxidation and membrane damage [18]. This results in the organelle's death [19, 20]. A previous study has shown growth sensitivity differences to paraquat exposure for cyanobacteria and green algae [21]. Nestler et al. concluded that the mode of action of paraquat was reflected in the differing responses of multiple endpoints in green alga [8]. However, research relating the mechanisms of sensitivity differences between cyanobacteria and green algae is not well explored. *Microcystis* is a cyanobacterium species which related to harmful algal blooms in worldwide freshwater ecosystems, and *Chlorella* is a representative chlorophyte microalga in the aquatic system. In our pre-screening test, we found that the *Microcystis* and *Chlorella* are the most sensitive species and the most tolerance species for paraquat, respectively (data were not shown). Thus, in the present study, we elucidated the mechanisms of sensitivity differences of these two representative species, one of which, *Microcystis aeruginosa* (Kützing) Kützing, is a prokaryote, and the other, *Chlorella* sp., is a eukaryote. Multiple endpoints were measured at different time scales following acute and chronic exposure. Acute effects were defined as occurring within 24 h (shorter than one cell division under the growth conditions used) [17] and assessed by measuring the response of photosynthetic processes. Chronic toxicity was measured after 96 h (longer than one reproduction cycle under the growth conditions used) [17], using antioxidant enzyme biomarkers, indicators of oxidative stress, photosynthetic processes, and morphological characters as the endpoints.

Materials and methods

Test organisms and culture condition

Eight species and strains of *Microcystis* spp. and seven species and strains of *Chlorella* spp. were tested in preliminary microplate assays. Detailed information is presented in Additional file. All the strains were provided by the Freshwater Algae Culture Collection at the Institute of Hydrobiology, Chinese Academy of Sciences (FACHB-Collection; Wuhan, China). The results of preliminary experiments showed that paraquat was more toxic to *Microcystis* than to *Chlorella.* Based on preliminary results, axenic strains of *M. aeruginosa* FACHB-469 and *Chlorella* sp. FACHB-1512 were selected. Cells were cultivated in BG11 medium at 25 ± 1 °C, and illuminated at white cool fluorescent light lamps (35 μmol photons m^{-2} s^{-1}), with a light/dark cycle of 12 h: 12 h. The cultures were manually shaken 3 or 4 times each day during incubation.

Experimental design

Three hundred millilitres of BG11 medium spiked with 0 (control), 0.001, 0.01, 0.02, 0.05, 0.1, 0.2, 0.5, and 1 mg L^{-1} paraquat for *M. aeruginosa* and 0.1, 0.2, 0.5, 1, 5, 10, and 30 mg L^{-1} for *Chlorella* sp. was added to 500 mL Erlenmeyer flasks ($n = 3$). Paraquat (99.7%) was obtained from Macklin (Shanghai, China) and a stock solution made by dissolving 2 g in 1 L of sterile deionized water. The stock solution was stored at 4 °C. Treatment concentrations were established from the preliminary toxicity tests described above which are shown in Additional file 1: Fig. S2. Flasks were inoculated with log-phase cells to an initial cell density of 2.0×10^6 cells mL^{-1} and 1.2×10^6 cells mL^{-1} for *M. aeruginosa* and *Chlorella* sp., respectively. All the cultures were incubated for 96 h under the conditions as described above.

Measurement of the endpoints

Endpoints for growth performance

The growth performance was quantified via a commonly used method [17]. After each 24 h interval, optical density (OD_{680}) was measured by in UV spectrophotometer (Shimadzu, Kyoto, Japan).

Endpoints for photosynthetic processes

To test the effect of acute exposure (5 min, 1 h, 3 h, 5 h, 9 h, and 24 h) on photosynthetic processes, polyphasic Chl *a* fluorescence transients were measured using a Handy-Plant Efficiency Analyzer (Handy-PEA, Hansatech, UK) with an actinic light of 3000 μmol photons m^{-2} s^{-1}. All samples were dark-adapted for 10 min before measurement. The fluorescence signals were recorded within a time period from 10 μs to 2 s, and fluorescence kinetics showed a polyphasic rise over time known as the O–J–I–P transients [22]. The initial fluorescence level O, corresponds to the minimal Chl *a* fluorescence yield with all PSII reaction centers open, while the J–I transient is caused by the gradual reduction of primary electron acceptors, Q_A and Q_B. The P level is the maximal fluorescence yield (F_M) when there is an accumulation of Q_A-Q_B^{2-} [22, 23]. To better analyze the Chl *a* fluorescence differences between the treatments for different concentrations and exposure times, a total of 10 parameters were evaluated during the JIP test, as shown in Table 1, which shows the PSII energy fluxes [24, 25]. The data are presented as percentages of the corresponding control values, and their absolute value changes were plotted as a radar map. In addition, the maximum quantum yield for primary photochemistry (F_v/F_m) and the maximum relative electron transport rate ($rETR_{max}$) were analyzed daily by a Water–PAM fluorescence monitoring system (Walz, Effeltrich, Germany). All samples were dark-adapted for 10 min before measurement. The minimum fluorescence

Table 1 JIP test parameters with explanations and formulae calculated using data extracted from the O-J-I-P fast fluorescence transient following the equations of Strasser and Strasser [24]

Parameter and formulae	Description
$V_J = (F_{2ms} - Fo)/(Fm - Fo)$	Relative variable fluorescence intensity at the J-step, reflecting the open state of reaction centers
$\varphi_{Eo} = ETo/ABS = [1 - (Fo/Fm)] \cdot \psi_0$	Quantum yield for electron transport (at $t = 0$)
$\psi_0 = ET_O/TR_O = (1 - V_J)$	Probability that a trapped excitation transfers an electron into the electron transport chain beyond Q_A (at $t = 0$)
$RC/CSo = \varphi_{Po} \cdot (V_J/Mo) \cdot (ABS/CSo)$	Number of RCs per CS, reflecting density of RCs
$ABS/RC = Mo \cdot (1/V_J) \cdot (1/\varphi_{Po})$	Absorption flux per reaction center (RC)
$ETo/RC = Mo \cdot (1/V_J) \cdot \Psi o$	Electron transport flux per RC (at $t = 0$)
$DIo/RC = ABS/RC - TRo/RC$	Dissipated energy flux per RC (at $t = 0$)
$TRo/RC = Mo \cdot (1/V_J)$	Trapped energy flux per RC (at $t = 0$)
$PIabs = (RC/ABS) \cdot [\varphi_{Po}/(1 - \varphi_{Po})] \cdot [\Psi o/(1 - \Psi o)]$	Performance index based on absorption of light energy
$\Phi p_0 = TRo/ABS = 1 - (Fo/Fm)$	The maximum photochemical efficiency (at $t = 0$)

(F_0) and the maximum fluorescence (F_m) were measured under a low light intensity and a saturating light pulse, respectively. F_v/F_m can be derived from the equations $F_v/F_m = (F_m - F_0)/F_m$. The EC_{50} values based on F_v/F_m for different exposure time were calculated according to the method of Franz et al. [16]. The rapid light curve (RLC)—indicating the electron transport responses to increasing irradiance—were then plotted, and $rETR_{max}$ was calculated according to the relative value of the plateau phase in RLC. During plotting RLC, 10 steps of actinic irradiance (0, 24, 124, 188, 276, 420, 625, 885, 1224, and 1427 μmol photons m^{-2} s^{-1}) were included with a 20 s interval time between each adjacent step.

Endpoints for oxidative stress

For anti-oxidant relevant enzyme measurements, 40 mL cell suspensions of all treatments were centrifuged (4500×*g*, 4 °C) at the end of the bioassay (96 h) and washed twice with deionized water. The pellets were resuspended in 2 mL of 50 mM sodium phosphate buffer (PBS, pH 7.8). Cells were homogenized by the Continuous High-Pressure Cell Disrupter (with 0.2 mm zirconium beads) and then centrifuged (6000×*g*, 4 °C, for 10 min). The supernatant was used for biochemical analysis. Total soluble protein was measured using the BCA Protein Assay Kit (Beyotime, China). The concentration of malodialdehyde (MDA)—a lipid peroxidation index—was analyzed using the thiobarbituric acid-reacting substance method [26]. SOD activity was analyzed by monitoring the inhibition of the photochemical reduction of nitroblue tetrazolium (NBT) according to Dhindsa and Matowe [27]. CAT activity was determined according to Aebi [28].

The ROS level in cells was measured after 96 h exposure using the cell permeable indicator 2′, 7′-dichlorodihydrofluorescein diacetate (DCFH-DA) (Sigma, St. Louis, Missouri, USA), according to the method described by Cheng et al. [29]. A final concentration of 10 μM DCFH-DA was added to the samples which were incubated at 25 °C in the dark for 1 h. Fluorescence was measured using a flow cytometer (FACS Verse BD Biosciences, Franklin Lakes, New Jersey, USA) with excitation and emission wavelengths of 488 nm and 525 nm, respectively. Data are expressed as a percentage of the respective control values and are presented as mean ± SE of the mean.

Endpoints for cell-membrane integrity

Cell-membrane integrity was assessed by SYTOX™ Green Ready Flow™ Reagent (Life Technologies, Carlsbad, California, USA) after 96 h of exposure to paraquat. As a cell-impermeant dye, SYTROX Green enters the cell after loss of membrane integrity and binds with DNA to produce a bright green fluorescent complex which can be used to distinguishing plasma membrane damaged cells from integrated membrane cells in flow cytometry assays [30]. Two drops of reagent were added to 1 mL of the sample containing 10^6 cells mL^{-1} and the sample was incubated for 15 min in the dark at room temperature. The fluorescence was analyzed by flow cytometry with excitation and emission wavelengths of 488 nm and 523 nm, respectively, and data were presented as the percentage of cells that were stained with SYTOX™ green.

Endpoints for submicroscopic structure

At the end of the assays, the morphological effects of paraquat were determined in cells exposed to 0.1 mg L^{-1} and 1 mg L^{-1} and compared to the controls. Cells were collected by centrifugation (2000×*g* for 5 min) and fixed overnight at 4 °C with 2.5% glutaraldehyde. The pellets were washed three times for 15 min with phosphate buffer solution (0.1 M, pH 7.0) and then post-fixed with 1% osmium tetroxide for 2.5 h. Samples were dehydrated through a series of ethanol washes (30, 50, 70, 80, 90, and 100%, consecutively) for 10 min at each step and then transferred to absolute acetone for 20 min. Samples were then placed in a 2:1 mixture of absolute acetone: final resin for 1 h at room temperature then transferred to a 1:2 mixture of absolute acetone: final resin overnight, and finally into 100% final resin mixture for 1 h. Samples were then embedded in 100% EPON 812 resin (37 °C for 12 h) and heated at 60 °C for 48 h. Ultrathin sections (70 nm) were obtained with a Leica EM UC7 ultramicrotome contrasted with uranyl acetate and lead citrate and observed in a transmission electron microscope (Hitachi-7700, Hitachi, Tokyo, Japan) using an acceleration voltage of 80 kV.

Data analysis and statistics

All data are presented as mean ± standard error (SE). Flow cytometric analysis data were analyzed using FlowJo software (Tree Star Software, San Carlos, California, USA). One-way analysis of variance (ANOVA), followed by least-significant difference (LSD) (for homogeneity of variance), or Dunnett's two-sided comparison test (for heterogeneity of variance) was applied to determine statistical differences between the different endpoints for different paraquat treatments and the control for each species. Independent sample *t* tests were performed to compare the *M. aeruginosa* and *Chlorella* sp. responses following exposure at the same paraquat concentration. Differences were considered to be significant at $p < 0.05$ unless otherwise stated.

Results

Distinct growth patterns of *M. aeruginosa* and *Chlorella* sp. following exposure to paraquat

Figure 1 shows dose- and time-dependent patterns of microalgal growth under paraquat exposure for both *M. aeruginosa* and *Chlorella* sp. Compared to the control, the growth of *M. aeruginosa* was significantly inhibited at concentrations of 0.2, 0.5, and 1 mg L^{-1} ($p < 0.01$, Fig. 1a). For *Chlorella* sp., growth inhibition was observed at concentrations of 5, 10, and 30 mg L^{-1} ($p < 0.01$, Fig. 1b), with inhibition rates of 39.85, 60.19, and 79.58%, respectively. Besides, the growth of *M. aeruginosa* was lower at 0.5 and 1 mg L^{-1} during the acute exposure stage (24 h, Fig. 1a), while for *Chlorella* sp., the declining growth curve was observed at 30 mg L^{-1} until 72 h (Fig. 1b).

Acute responses after exposed to paraquat

The fluorescence kinetics of *M. aeruginosa* and *Chlorella* sp. exposed to paraquat for 24 h are shown in Fig. 2. The fluorescence yield is presented as the concentration-dependent response of each species over 24 h. A concentration-dependent increase in the fluorescence yield was found in *M. aeruginosa* exposed to paraquat at concentrations higher than 0.1 mg L^{-1} (Fig. 2a). Conversely, a concentration-dependent decrease in the fluorescence yield was observed in *Chlorella* sp. at concentrations higher than 0.5 mg $^{-1}$ with the lowest yield found in cultures exposed to 30 mg L^{-1} (Fig. 2b). When the fluorescence kinetics were plotted as the relative variable fluorescence to better reveal the changes in the transients (Fig. 2a, b, inserts), an increase in the J transient was found for *M. aeruginosa* at concentrations greater than 0.2 mg L^{-1} (Fig. 2a, inserts).

Chl*a* fluorescence for each species changed in a concentration and time-dependent manner within 24 h (Fig. 3). Increases in V_j, ABS/RC, DI_o/RC, and TR_0/RC and decreases in ET_0/RC, RC/CS_o, ψ_0, ϕ_{Eo}, and ϕ_{P0} were observed for both strains. Figure 3c shows significant changes in chlorophyll fluorescence after 3 h for *M. aeruginosa* at 1 mg L^{-1} ($p < 0.05$) and for *Chlorella* sp. after 9 h exposure at 30 mg L^{-1} (Fig. 3k). In addition, the PI_{abs} index (Performance index based on absorption of light energy) decreased in a concentration-dependent manner after only 5 min for both *M. aeruginosa* (> 0.001 mg L^{-1}) and *Chlorella* sp. (> 5 mg L^{-1}). Similarly, a significant decrease in $rETR_{max}$ was observed at concentrations of 0.2 mg L^{-1} and higher for *M. aeruginosa,* and for *Chlorella* sp. at concentrations of 10 mg L^{-1} ($p < 0.05$) and higher (Fig. 4).

The EC_{50} based on F_v/F_m values decreased significantly with exposure time (Fig. 5). After 5 h cumulative exposure, the EC_{50} for *M. aeruginosa* was 0.54 mg L^{-1}, while for *Chlorella* sp., it was higher at 44.76 ± 3.13 mg L^{-1} after 24 h.

Chronic responses after exposed to paraquat

To better explain the paraquat sensitivity variation between these two species, biochemical parameters were measured after 96 h of chronic exposure. Figure 6a shows that F_v/F_m and $rETR_{max}$ were lower for *M. aeruginosa* when the exposure concentration was 0.2 mg L^{-1} or higher, but for *Chlorella* sp., Figure 6b shows that $rETR_{max}$ was only lower when the exposure concentration exceeded 5 mg L^{-1}.

Tables 2 and 3 show that the enzymatic activities of CAT and SOD for each strain were significantly differently between treatments ($p < 0.01$). Significantly higher CAT and SOD activities were measured in *M. aeruginosa* when exposure concentrations exceeded 0.1 mg L^{-1} and for *Chlorella* sp. when they exceeded 1 mg L^{-1}.

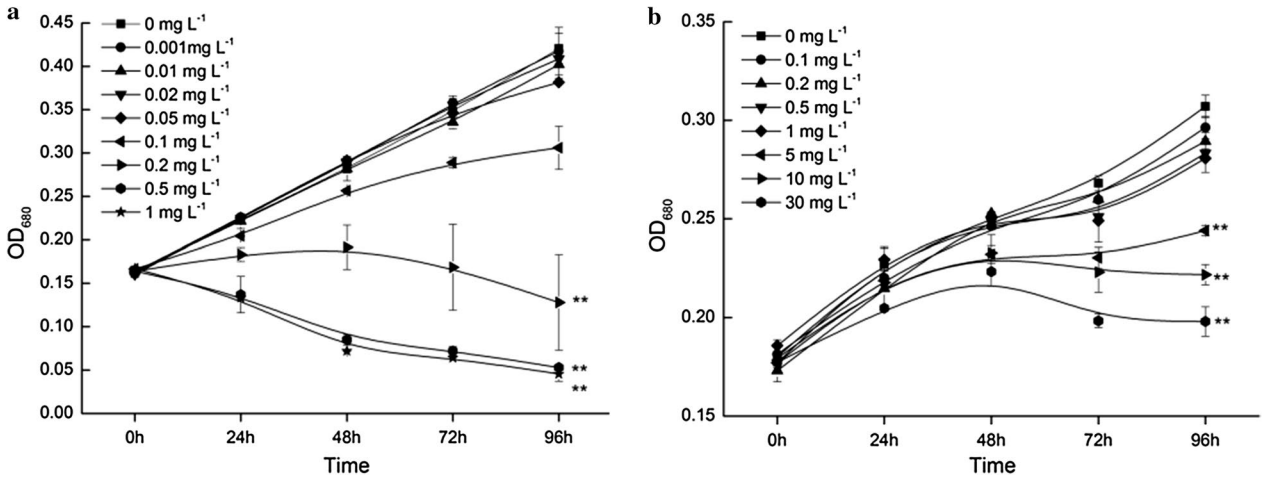

Fig. 1 96 h population growth curves exhibited by optical density at 680 nm (OD_{680}) in flask assays. **a** *Microcystis aeruginosa* and **b** *Chlorella* sp. Error bars are mean ± SE. $^{**}p < 0.01$

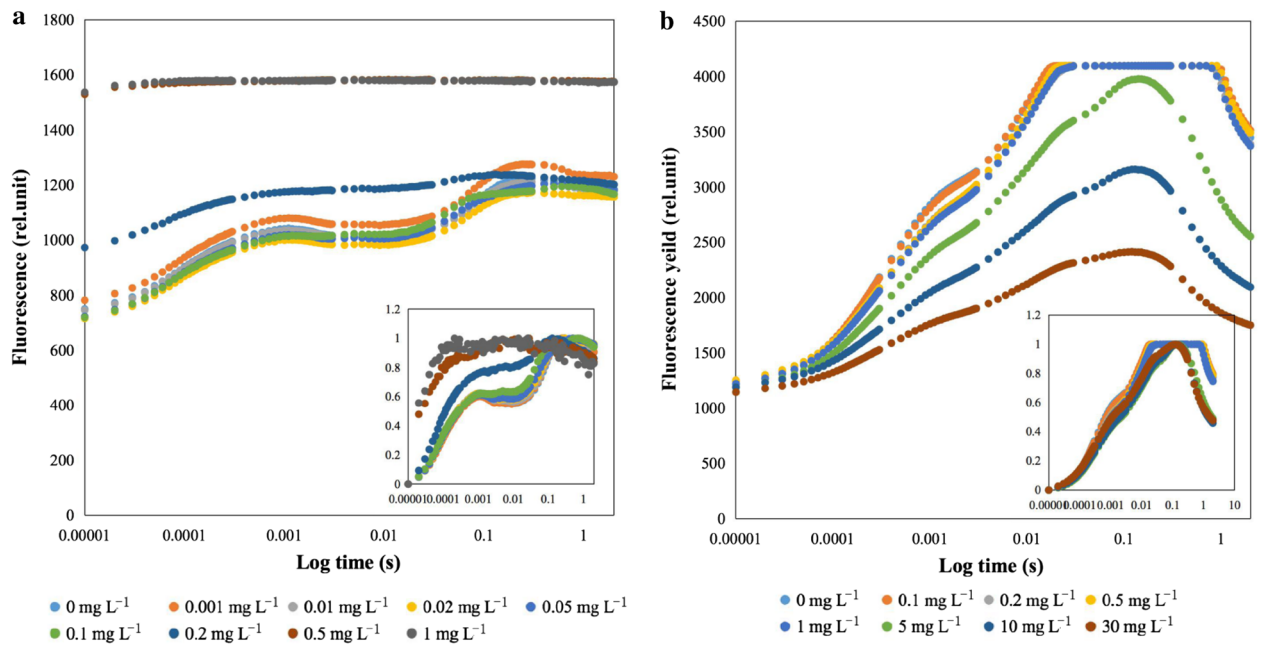

Fig. 2 Rapid rise fluorescence kinetics after 24 h exposure to paraquat. Inserts—the same kinetics are shown as normalized O–J–I–P transient curves. **a** *Microcystis aeruginosa* and **b** *Chlorella* sp

(See figure on next page.)

Fig. 3 Radar plots of the main OJIP fluorescence parameters following exposure at 5 min, 1 h, 3 h, 5 h, 9 h, and 24 h for *Microcystis aeruginosa* (**a**–**f**) and *Chlorella* sp. (**g**–**l**). The value in the plots is the ratio of the treatment to the control. The descriptions of fluorescence parameters are presented in Table 1

Significantly elevated MDA content ($p < 0.05$) was only observed in *Chlorella* sp. at a paraquat concentration of 1 mg L^{-1} (Table 3).

The relative results (control = 100%) for ROS and SYTRO green are presented in Fig. 7. For *M. aeruginosa*, significantly enhanced production of ROS occurred in cells, where exposure concentration was 0.2 mg L^{-1} or higher and the percentage of membrane damaged cells was around 20 times higher than the control at exposure concentrations greater than 0.2 mg L^{-1} after 96 h ($p < 0.05$). Conversely, for *Chlorella* sp., elevated ROS and membrane-damaged cells only occurred at exposure concentrations of 5 mg L^{-1} or higher and only around double that of the control.

The ultrastructure of both species exposed to two concentrations of paraquat for 96 h was compared using transmission electron microscopy (TEM) (Figs. 8, 9). For *M. aeruginosa*, the thylakoids and cytoplasm were shown to be distorted, and the cell walls damaged and detached from the cytoplasmic membrane in the 0.1 mg L^{-1} treatment (Fig. 8d–f), while in the 1.0 mg L^{-1} treatment, thylakoid membrane stacks, cytoplasmic vacuolation, and cytoclasis were evident (Fig. 8g–i). For *Chlorella* sp., the ultrastructures of cells were similar to the control treatment (Fig. 9a–c) for both 0.1 and 1.0 mg L^{-1} treatments, except that several outermost layers of the multi-layered cell walls appeared disrupted, and a disarrangement of organelles within cells was observed at in the 1.0 mg L^{-1} treatment (Fig. 9d–i).

Discussion

This study investigated the sensitivity differences to paraquat of two phytoplankton species *M. aeruginosa* and *Chlorella* sp. using time-dependent multi-endpoint assays. In general, *M. aeruginosa* was found to be tenfold more sensitive than *Chlorella* sp. to both chronic and acute exposures. These include photosynthetic processes, antioxidant response, oxidative stress, sub-microstructure changes, and growth inhibition.

Photosynthesis is a key physiological process for phototrophic organisms and is very sensitive to pollutants through the effects that some pollutants have on the electron transport chain [31, 32]. Chl *a* fluorescence is a rapid and non-invasive method for monitoring cellular stress and is commonly used to assess and quantify phytotoxicity in phytoplankton [32–35]. In the present study,

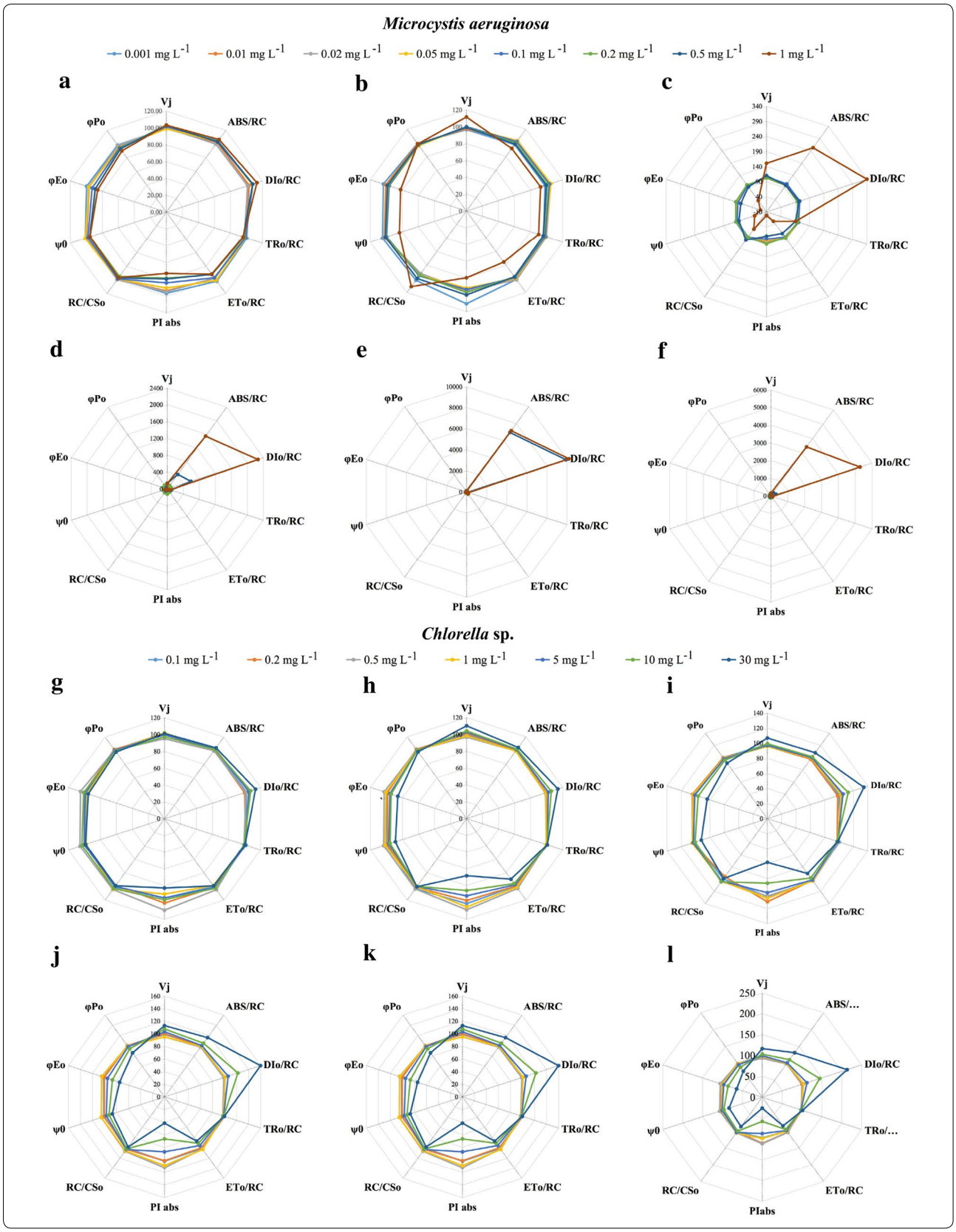
Microcystis aeruginosa
0.001 mg L-1
0.01 mg L-1
0.02 mg L-1
0.05 mg L-1
0.1 mg L-1
0.2 mg L-1
0.5 mg L-1
1 mg L-1
a
b
c
d
e
f
Chlorella sp.
0.1 mg L-1
0.2 mg L-1
0.5 mg L-1
1 mg L-1
5 mg L-1
10 mg L-1
30 mg L-1
g
h
i
j
k
l
Vj
ABS/RC
DIo/RC
TRo/RC
ETo/RC
PI abs
RC/CSo
ψ0
φEo
φPo
ABS/...
TRo/...
PIabs

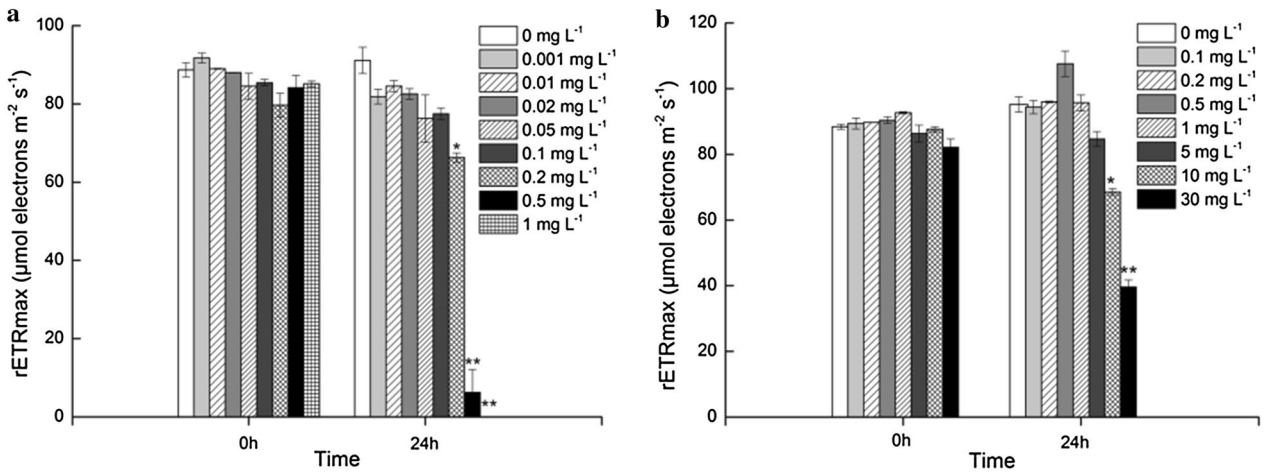

Fig. 4 Effect of paraquat on the maximum relative electron transport rate ($rETR_{max}$) for **a** *Microcystis aeruginosa*, and **b** *Chlorella* sp. at 0 h and 24 h. Error bars are mean ± SE

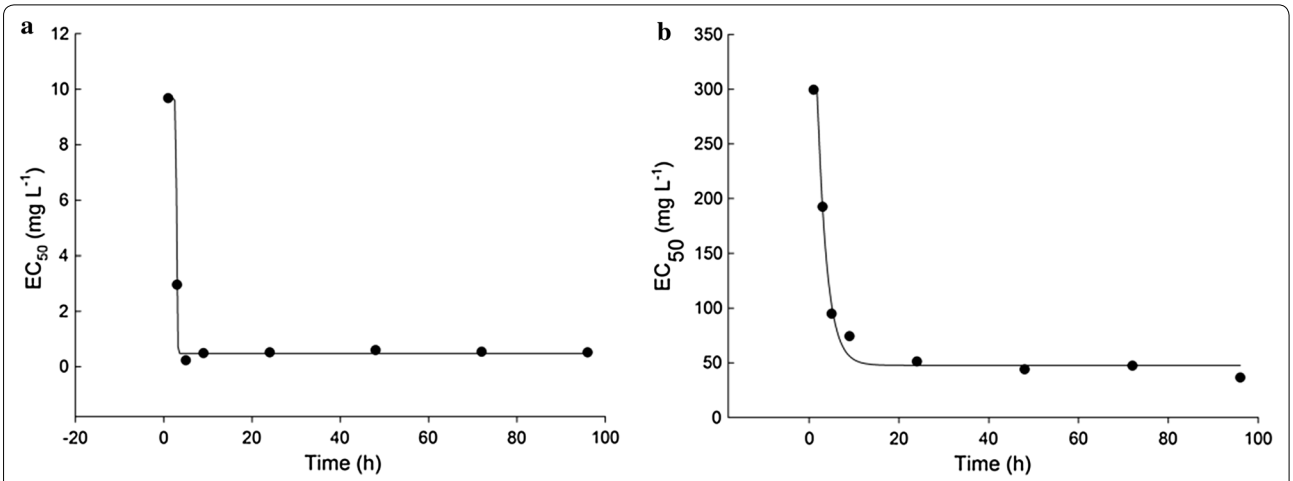

Fig. 5 EC_{50} values based on the maximum quantum yield (F_v/F_m) following cumulative exposure time arising from concentration–response curves for **a** *Microcystis aeruginosa* and **b** *Chlorella* sp

the fluorescence yield is presented as the acute concentration-dependent response of *M. aeruginosa* and *Chlorella* sp. (Fig. 2) and shows that paraquat affected PSII photochemistry of both species [36]. Hess previously showed that the phytotoxic action of paraquat is based on interference with photosynthetic electron transport in PSI [18]. PSII is connected to PSI via the cytochrome b6/f complex [37], so if electron transfer from PSI is inhibited, PSII photochemistry would also be affected. In addition, the previous research has shown that paraquat caused up-regulation of the central component of PSII (D1 protein) in *Chlamydomonas reinhardtii* P.A.Dangeard [38].

The O–J–I–P fluorescence kinetics shows an increase at the J transient for both species after 24 h exposure to paraquat (Fig. 2, Insert). This indicates that paraquat appears to block electron transfer from Q_A to Q_B in both species. The similarity of the Chl *a* fluorescence response to paraquat in both species showed that the mode of action in PSII was similar. The absorption flux per reaction center (ABS/RC), which in a measure of PSII antennae size, was increased and may indicate an inactivation of PSII reaction centers by paraquat [25, 34, 39]. A concomitant decrease of ET_0/RC indicated that the re-oxidation of Q_A through electron transport was reduced. Both species showed a decrease in ψ_0 (the probability that an electron residing on Q_A enters the electron transport chain) and an increase in the J transient (V_j), thus confirming that electron transport was blocked between Q_A and Q_B (Fig. 3e, j). Similar results were found for other herbicides, including atrazine, diuron, and hexazinnone

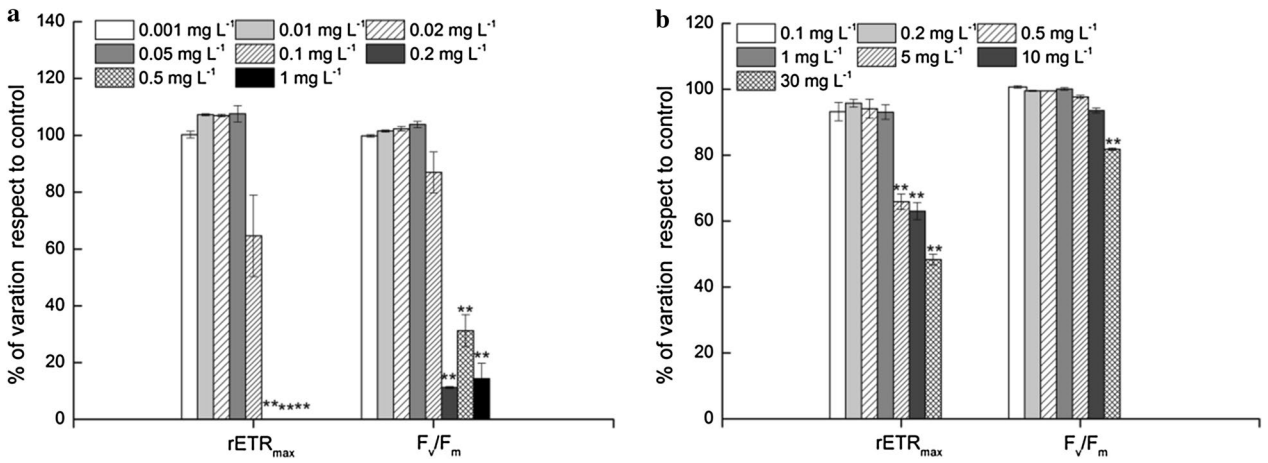

Fig. 6 Difference of $rETR_{max}$ and F_v/F_m following chronic exposure for **a** *Microcystis aeruginosa* and **b** *Chlorella* sp. Values are relative to the control and significant differences are indicated by an asterisk (*). Error bars are mean ± SE

Table 2 Antioxidant enzymes biomarkers in *M. aeruginosa* exposed to different paraquat concentrations

	Paraquat (mg L^{-1})								
	0.00	0.00	0.01	0.02	0.05	0.10	0.20	0.50	1.00
MDA (U mg^{-1} protein)	1.34 ± 0.07	1.27 ± 0.03	1.39 ± 0.07	1.24 ± 0.03	1.29 ± 0.07	1.37 ± 0.02	1.41 ± 0.23	1.50 ± 0.27	1.72 ± 0.00
CAT (U mg^{-1} protein)	20.58 ± 1.37	22.72 ± 1.13	25.59 ± 0.36	24.07 ± 0.544	29.61 ± 1.17	37.86 ± 3.55**	200.31 ± 40.34**	242.21 ± 3.55**	260.20 ± 27.02**
SOD (U mg^{-1} protein)	49.04 ± 5.31	56.29 ± 3.60	65.07 ± 1.00	59.57 ± 2.64	71.73 ± 3.85	88.80 ± 4.68*	208.41 ± 38.59**	406.55 ± 7.30**	436.80 ± 63.22**

Average values ± SE ($n = 3$). *$p < 0.05$

Table 3 Antioxidant enzymes biomarkers in *Chlorella* sp. exposed to different paraquat concentrations

	Paraquat (mg L^{-1})							
	0.00	0.10	0.20	0.50	1.00	5.00	10.00	30.00
MDA (U mg^{-1} protein)	1.68 ± 0.06	1.75 ± 0.15	1.96 ± 0.11	1.76 ± 0.02	3.32 ± 0.70**	2.50 ± 0.05	2.15 ± 0.61	1.61 ± 0.10
CAT (U mg^{-1} protein)	31.41 ± 2.10	36.22 ± 1.07	47.77 ± 5.29*	42.64 ± 2.43	50.16 ± 5.86*	52.45 ± 3.30**	65.85 ± 3.06**	91.03 ± 9.54**
SOD (U mg^{-1} protein)	82.46 ± 7.06	92.82 ± 1.53	124.89 ± 12.91*	104.36 ± 4.62	120.30 ± 9.73*	131.93 ± 8.17**	135.59 ± 3.67**	189.08 ± 24.30**

Average values ± SE ($n = 3$). *$p < 0.05$

[33, 40, 41]. Furthermore, as shown in Fig. 3a, f, the PI_{abs} index decreased in a concentration-dependent manner after only 5 min of exposure to paraquat for both species, indicating that PI_{abs} is a sensitive indicator of early response to paraquat exposure.

Although the mode of action of paraquat towards each of the two species was similar, the toxicokinetic and toxicodynamic processes were different. In the present study, acute responses (i.e., within 24 h) such as the effect on chlorophyll fluorescence in cyanobacterial cells occurred within 3 h of exposure ($p < 0.05$; Fig. 3c). Higher acute susceptibility in PI_{abs}, $\phi_{Eo,}$ and ψ_0 was found for *M. aeruginosa* with effects becoming evident within hours of exposure, but not for *Chlorella* sp. until after 24 h for the same concentrations (1.0 mg $^{-1}$). In addition, the EC_{50} based on F_v/F_m for *M. aeruginosa* was lower than for *Chlorella* sp. and was obtained after only 5 h exposure (Fig. 5). Unlike *Chlorella* sp., a decrease of $rETR_{max}$ was observed in *M. aeruginosa* after 24 h following exposure to paraquat at concentrations of 0.2 mg L^{-1} and higher

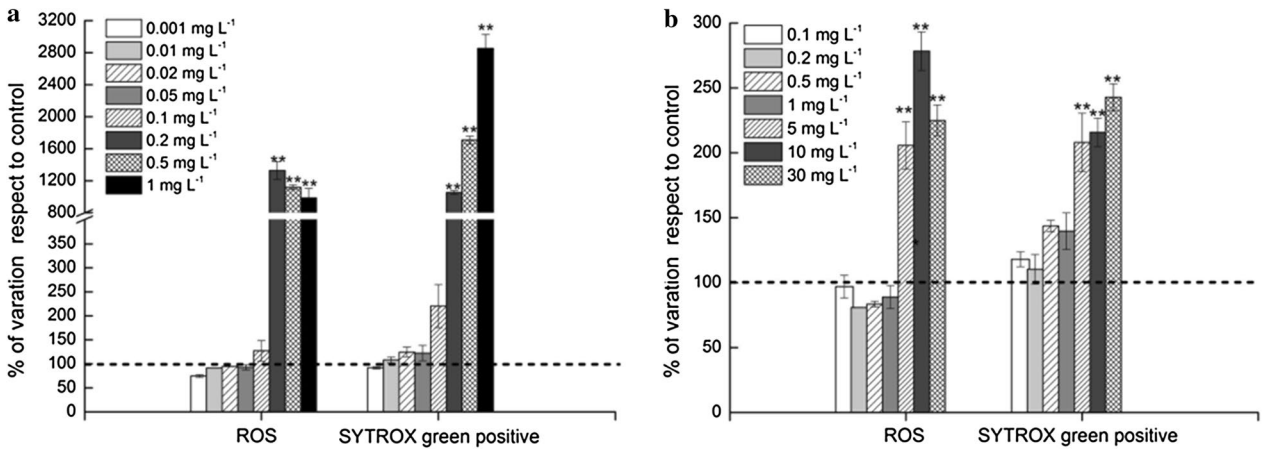

Fig. 7 Difference of ROS level and SYTRO green positive following chronic exposure for **a** *Microcystis aeruginosa* and **b** *Chlorella* sp. Values are relative to the control and significant differences are indicated by an asterisk (*). Error bars are mean ± SE

(Fig. 4). This shows that the electron transport chain of *M. aeruginosa* was adversely affected by paraquat at relatively low concentrations, and photosynthetic responses to paraquat stress were significantly different between *M. aeruginosa* and *Chlorella* sp. As a result, growth inhibition of *M. aeruginosa* in this study occurred during the acute exposure stage (Fig. 1). Collectively, photosynthetic parameters can be used as sensitive cellular endpoints to study the early effects of paraquat on algae [8]. Our results provide supplementary evidence for differences in paraquat sensitivity between *M. aeruginosa* and *Chlorella* sp. in acute response.

The results of chronic response also showed sensitivity difference between the two species. One of the reported toxicity mechanisms for paraquat is its effect on cyclic reduction–oxidation reactions, through which reactive oxygen species (ROS) are induced in unicellular alga [42, 43]. SOD, peroxidase (POD), and CAT activities increased in response to paraquat exposure to remove excessive ROS [44–46]. Similarly, in the present study, significant increases in CAT and SOD activities were observed in *M. aeruginosa* after 96 h exposure to paraquat concentrations greater than 0.1 mg L^{-1} compared to the control (Table 2), whereas for *Chlorella* sp., a similar sensitivity was only found at paraquat concentrations of 1 mg L^{-1} or higher (Table 3). Nevertheless, the results of intracellular ROS levels and MDA content showed that the cells were still oxidatively damaged. An increase of intracellular ROS levels (Fig. 7) and MDA content (Tables 2, 3) was observed in *M. aeruginosa* at the 0.2, 0.5, and 1.0 mg L^{-1} treatments and in *Chlorella* sp. at 5, 10, and 30 mg L^{-1} treatments, respectively. The number of membrane damaged cells also increased significantly in *M. aeruginosa* at concentrations greater than 0.2 mg L^{-1} and in *Chlorella* sp. at concentrations greater than 5 mg L^{-1} (Fig. 7). This indicates that the cellular antioxidant defense mechanisms might not be capable of adequately protecting the cells following exposure to higher paraquat concentrations [8, 10]. Overproduction of ROS could trigger oxidative damage to proteins, nucleic acids, and lipids, and lead to the disruption of cellular structures, resulting in morphological changes and cell death [47, 48]. It could also explain the significantly higher growth inhibition at these concentrations, as shown in Fig. 1.

Interestingly, there were also several differences in the anti-oxidative responses of these two species. First, as shown in Tables 2 and 3, the response of the antioxidant systems was significantly different ($p < 0.01$). At exposure levels which caused significant growth inhibition for *M. aeruginosa* (> 0.2 mg L^{-1}) and *Chlorella* sp. (> 5 mg L^{-1}), the mean increase in CAT and SOD activity for *M. aeruginosa* cells was 11.25 and 7.14 times that of the control, whereas there was only 2.22 and 2.01 fold change in *Chlorella* sp. It has been reported that CAT and SOD vary among algal species when exposed under the same conditions to the same toxicant. For example, Martinez-Ruiz and Martinez-Jeronimo showed that 2, 4-dichlorophenoxyacetic acid (2, 4-D) induced a decrease of SOD activity, but did not affect the CAT activity in *M. aeruginosa*, while it produced significant differences compared to the control for *Ankistrodesmus falcatus* Corda Ralfs [49]. Second, compared to *Chlorella* sp., much higher increases in intracellular ROS levels and the percentage of membrane damaged cell were found for *M. aeruginosa* under the same treatment concentrations (i.e., 0.2, 0.5, and 1 mg L^{-1}, Fig. 7). Third, TEM images confirmed the results of oxidative damage from paraquat exposure at the ultra-structural level in both species. At the same

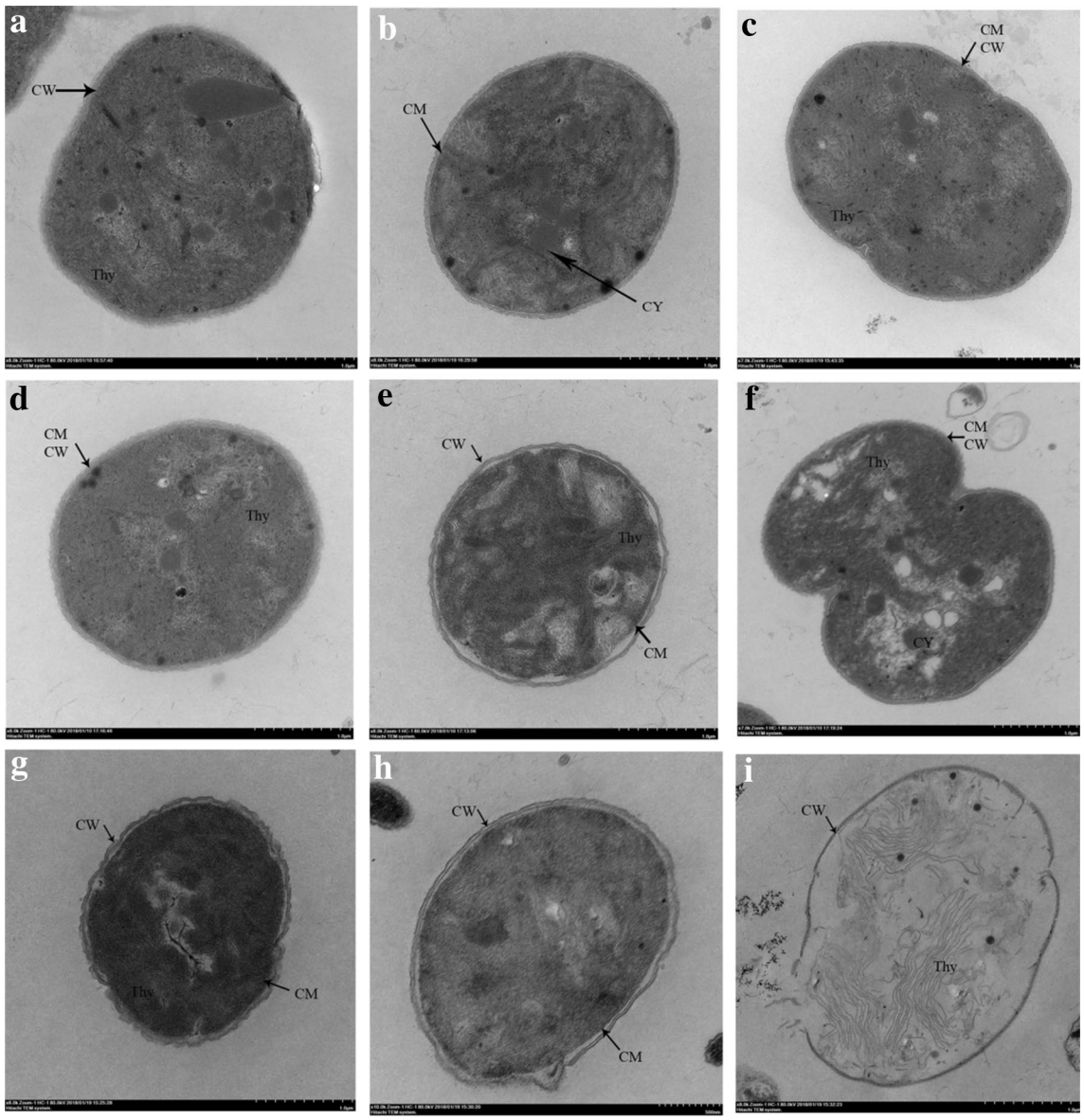

Fig. 8 TEM photomicrographs showing the ultrastructure of *Microcystis aeruginosa* following chronic exposure. **a**–**c** Control; **d**–**f** 0.1 mg L^{-1}; and **g**–**i** 1 mg L^{-1}. Thy, thylakoids; CW, cell wall; CM, cell membrane; Cy, cyanophycin

exposure concentrations, the morphological changes between the two species were also different. Therefore, paraquat can induce oxidative damage to both species but at different concentrations which depends on their sensitivity.

The similarity of the Chl *a* fluorescence response to paraquat in *M. aeruginosa* and *Chlorella* sp. indicated that the mode of action for paraquat in PSII was similar, that is, paraquat appears to block electron transfer from Q_A to Q_B in both species. However, the acute and chronic responses at the sub-cellular level showed that paraquat was more toxic to *M. aeruginosa* than to *Chlorella* sp. [21, 50]. Martinez-Ruiz and Martinez-Jeronimo suggested that differences in sensitivity could be related to species-specific responses [49]. There are at least four explanations for the species-specific responses to paraquat exposure observed in this study. First, the cell wall and cell membrane provide a self-protection barrier against xenobiotic chemicals, and this is different between the two species of phytoplankton. The cell envelope of *M. aeruginosa* (a prokaryote) is comprised of a cytoplasmic membrane, and a peptidoglycan layer composed of two sugar derivatives, N-acetylglucosamine and N-acetylmuramic acid, and several different amino

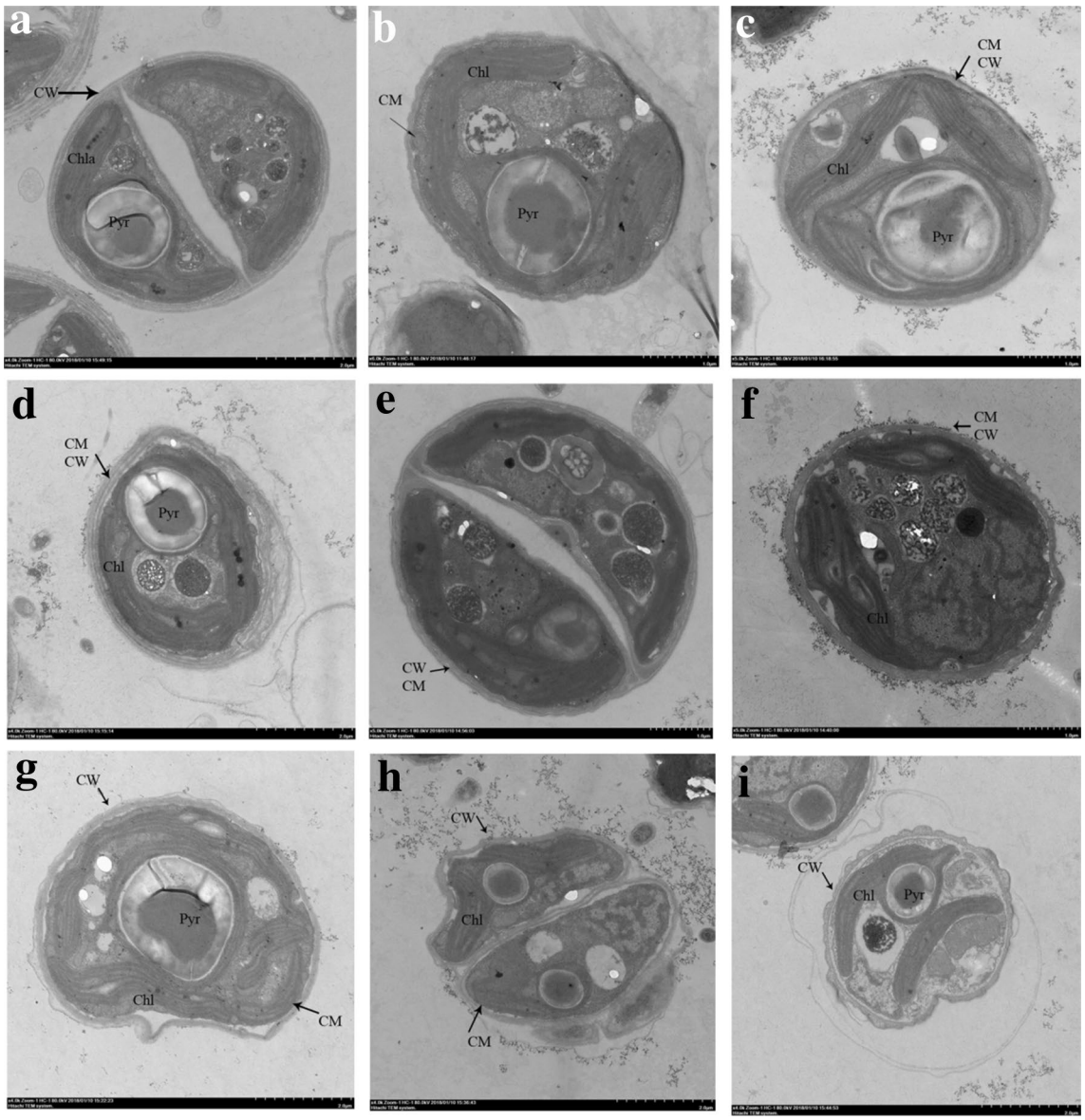

Fig. 9 TEM photomicrographs showing the ultrastructure of *Chlorella* sp. following chronic exposure. **a**–**c** Control; **d**–**f** 0.1 mg L^{-1}; and **g**–**i** 1 mg L^{-1}. Chl, chloroplast; CW, cell wall; CM, cell membrane; Pyr, pyrenoid

acids, as well as an outer membrane [51]. Conversely, the cell wall of *Chlorella* sp. (a eukaryote) is composed of microfibrillar layers and an outer component that was thicker (up to 166 μm) than *M. aeruginosa* (about 45 nm thick, Figs. 8, 9) [52]. A highly chemical resistant cell wall found in coccoid green algae including *Chlorella* sp. contains the biopolymer algaenan [53–55] and this may also contribute to a higher paraquat tolerance by *Chlorella* sp. compared to *M. aeruginosa*. Second, compared to cyanobacteria (where photosynthesis occurs in the cytoplasm), paraquat needs to pass through an additional double-membrane chloroplast envelope before it arrives at the thylakoid membranes in *Chlorella* cells [34]. Third, paraquat resistance of plant cells is determined by paraquat uptake and efflux, sequestration, and catabolism, and through detoxification of the reactive oxygen species

(See figure on next page.)

Fig. 10 Proposed mechanistic scheme for paraquat toxicity (1 mg L^{-1}) in *Microcystis aeruginosa* and *Chlorella* sp. The change of photosynthetic processes (Chl *a* fluorescence, $rETR_{max}$) and cell-membrane integrity (SYTRO green positive) in 24 h are defined as acute responses. The variation of oxidative stress (SOD, CAT, MDA, ROS), cell-membrane integrity (SYTRO green positive), and growth (OD_{680}) at 96 h are defined as chronic responses. Significant increased endpoints, significantly decreased endpoints, and no significant changed endpoints are presented in red, green, and dark blue, respectively

generated by paraquat [56]. Paraquat enters plant cells via a transport system that inherently functions as a transporter of polyamines which are structurally similar to paraquat [57, 58]. Incharoensakdi et al. proposed that the polyamine transport system in *Synechocystis* sp. PCC 6803 (which is a very rapid and energy-dependent process) is driven by a proton gradient and a membrane potential [59]. However, it is not universal, because studies on the green algae *C. reinhardtii* show that it does not contain short-living, high-affinity polyamine transporters [60]. Fourth, in comparison with eukaryotes, prokaryotes may have less elaborate enzymatic antioxidant pathways [34]. This may explain some of the sensitivity differences between cyanobacteria and green algae [61]. Esteves et al. showed that for atrazine, the sensitive strain decreased oxidative stress by increasing the activity of antioxidant enzymes such as SOD, but the tolerant strain invested in conjugation pathways and carotenoid maintenance [62]. Our results also showed that differences in response of the antioxidant system in the two species may explain differences in the extent of membrane and other ultrastructure damage. Therefore, differences between prokaryote and eukaryote physiology at the cellular level could contribute to the difference in toxicity, while the differences in inhibition efficiency might be largely dependent on the test species and incubation period. Y.

Conclusion

In this study, we found that paraquat affects population growth and photosynthetic processes, as well as inducing oxidative stress and anti-oxidative responses in two different types of phytoplankton, as shown in Fig. 10 (1 mg L^{-1} paraquat treatment as sample). For *M. aeruginosa*, Chl *a* fluorescence was affected after 3 h of exposure to paraquat. After a 96 h chronic exposure, significant increases in ROS levels, lipid peroxidation, growth inhibition, and the percentage of dead cells as well as comprehensive collapse of the cell structure occurred in *M. aeruginosa*. For *Chlorella* sp., only minimal effect on Chl *a* fluorescence was found following an acute exposure period (24 h), and after 96 h of chronic exposure to low concentrations of paraquat (< 1 mg L^{-1}), relative low levels of ROS and growth inhibition were observed. These results show that multiple endpoints measured for both acute and chronic exposures provide more comprehensive information about the sensitivity differences of *M. aeruginosa* and *Chlorella* sp. The difference in cell structure of the two species plays a pivotal role in their response to paraquat, suggesting that physiology differences between prokaryotes and eukaryotes need to be considered when the toxic effect of chemical pollutants is studied. This study provides a "departure point" to investigate the composition of phytoplankton communities under a potential selective pressure from an herbicide such as paraquat in a natural ecosystem.

Supplementary information

Supplementary information accompanies this paper at https://doi.org/10.1186/s12302-019-0255-4.

Additional file 1. The preliminary Microplate assay and the preliminary toxicity test for concentrations setting.

Abbreviation

ROS: reactive oxygen species; SOD: superoxide dismutase; CAT: catalase; PS I: photosystem I; F_M: the maximal fluorescence yield; F_v/F_m: the maximum quantum yield for primary photochemistry; $rETR_{max}$: the maximum relative electron transport rate; F_0: the minimum fluorescence; F_m: the maximum fluorescence; RLC: the rapid light curve; MDA: malodialdehyde; NBT: nitroblue tetrazolium; SE: standard error; ANOVA: one-way analysis of variance; LSD: least-significant difference; TEM: transmission electron microscopy; POD: peroxidase.

Acknowledgements

The authors thank Lingling Zheng (Freshwater Algae Culture Collection at the Institute of Hydrobiology, Chinese Academy of Sciences) for kind help in algal cultivation and Yan Wang (the Center for Instrumental Analysis and Metrology, Institute of Hydrobiology, Chinese Academy of Science) for technical assistance in flow cytometry The authors also thank Dr. Philip Orr and Dr. Sarah

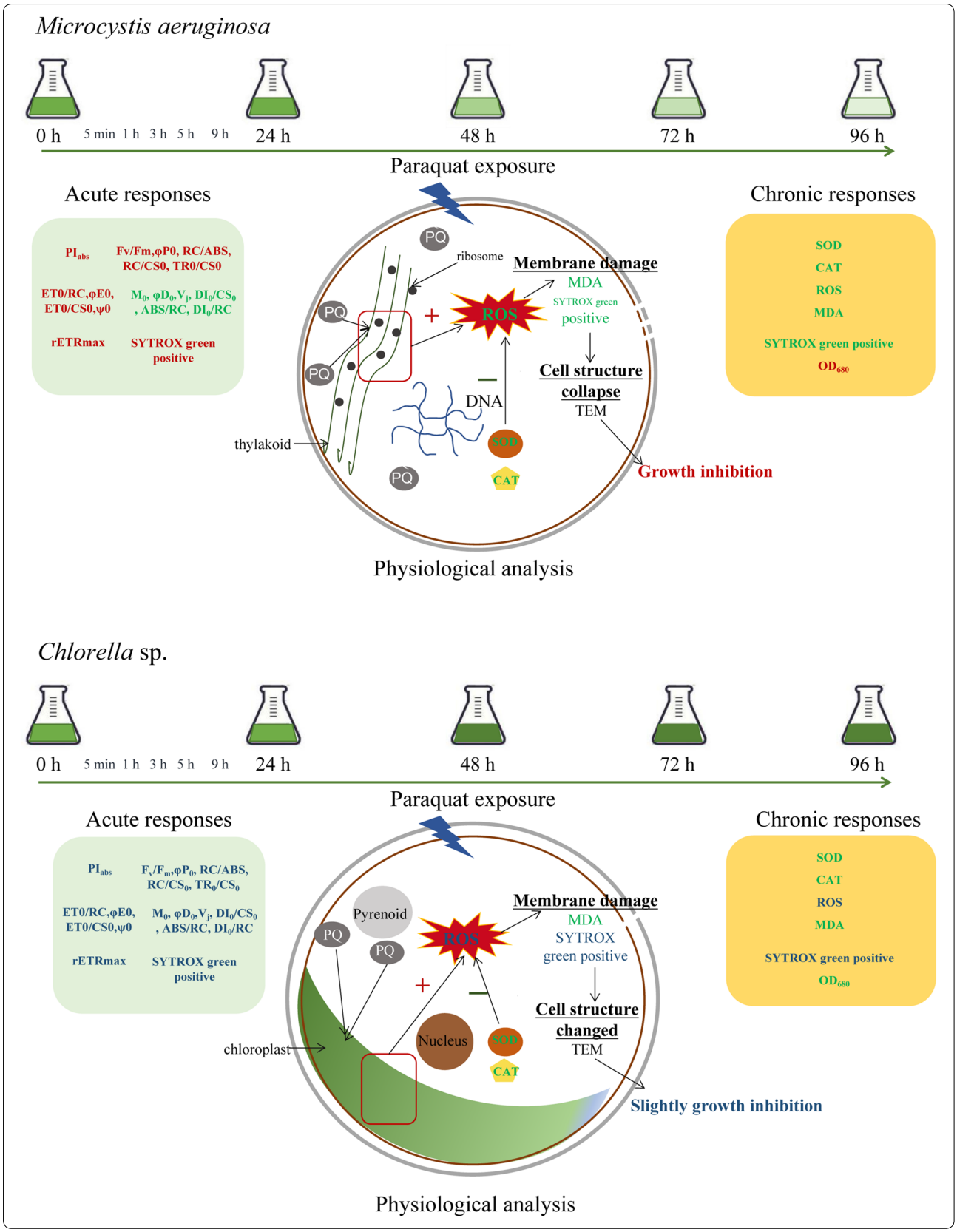
Microcystis aeruginosa
0 h
5 min 1 h 3 h 5 h 9 h
24 h
48 h
72 h
96 h
Paraquat exposure
Acute responses
PI$_{abs}$
Fv/Fm,φP0, RC/ABS, RC/CS0, TR0/CS0
ET0/RC,φE0, ET0/CS0,ψ0
M$_0$, φD$_0$,V$_j$, DI$_0$/CS$_0$, ABS/RC, DI$_0$/RC
rETRmax
SYTROX green positive
Chronic responses
SOD
CAT
ROS
MDA
SYTROX green positive
OD$_{680}$
PQ
ribosome
Membrane damage
MDA
SYTROX green positive
ROS
Cell structure collapse
TEM
DNA
thylakoid
SOD
CAT
Growth inhibition
Physiological analysis
Chlorella sp.
0 h
5 min 1 h 3 h 5 h 9 h
24 h
48 h
72 h
96 h
Paraquat exposure
Acute responses
PI$_{abs}$
F$_v$/F$_m$,φP$_0$, RC/ABS, RC/CS$_0$, TR$_0$/CS$_0$
ET0/RC,φE0, ET0/CS0,ψ0
M$_0$, φD$_0$,V$_j$, DI$_0$/CS$_0$, ABS/RC, DI$_0$/RC
rETRmax
SYTROX green positive
Chronic responses
SOD
CAT
ROS
MDA
SYTROX green positive
OD$_{680}$
Pyrenoid
PQ
ROS
Membrane damage
MDA
SYTROX green positive
Cell structure changed
TEM
Nucleus
chloroplast
SOD
CAT
Slightly growth inhibition
Physiological analysis

E. Crawford for their help with linguistic assistance of the manuscript and for suggesting useful changes.

Authors' contributions
BF, JY, and YC performed the experiments. BF, JY, and SL wrote the manuscript. LJ participated in the preliminary test. WZ contributed to the manuscript correction. All authors read and approved the final manuscript.

Funding
This work was supported by the National Key Research and Development Project (Nos: 2017YFE0125700 and 2018YFD0900701).

Availability of data and materials
The data sets supporting the conclusions of this article are included within the article and its additional file.

Ethics approval and consent to participate
Not applicable.

Consent for publication
Not applicable.

Competing interests
The authors declare that they have no competing interests.

Author details
[1] State Key Laboratory of Freshwater Ecology and Biotechnology, Institute of Hydrobiology, Chinese Academy of Sciences, Wuhan 430072, China. [2] University of Chinese Academy of Sciences, Beijing 100049, China. [3] Dalian Ocean University, Dalian 116023, China. [4] Key Laboratory of Eco-environments in Three Gorges Reservoir Region (Ministry of Education), Chongqing Key Laboratory of Plant Ecology and Resources Research in Three Gorges Reservoir Region, School of Life Science, Southwest University, Chongqing 400715, China.

Received: 10 July 2019 Accepted: 3 September 2019
Published online: 17 October 2019

References

1. Pesce S, Bouchez A, Montuelle B (2011) Effects of organic herbicides on phototrophic microbial communities in freshwater ecosystems. Rev Environ Contam Toxicol 214:87–124. https://doi.org/10.1007/978-1-4614-0668-6_5
2. El-Dib MA, Abou-Waly HF, El-Naby AMH (2000) Impact of pentachlorophenol on growth and community structure of Nile River water microalgae. Int J Environ Health Res 10:239–250. https://doi.org/10.1080/09603120050127185
3. Orvos DR, Versteeg DJ, Inauen J, Capdevielle M, Rothenstein A, Cunningham V (2002) Aquatic toxicity of triclosan. Environ Toxicol Chem 21:1338–1349. https://doi.org/10.1002/etc.5620210703
4. Ma JY (2005) Differential sensitivity of three cyanobacterial and five green algal species to organotins and pyrethroids pesticides. Sci Total Environ 341:109–117. https://doi.org/10.1016/j.scitotenv.2004.09.028
5. Dupraz V, Coquille N, Menard D, Sussarellu R, Haugarreau L, Stachowski-Haberkorn S (2016) Microalgal sensitivity varies between a diuron-resistant strain and two wild strains when exposed to diuron and irgarol, alone and in mixtures. Chemosphere 151:241–252. https://doi.org/10.1016/j.chemosphere.2016.02.073
6. Relyea RA (2005) The impact of insecticides and herbicides on the biodiversity and productivity of aquatic communities. Ecol Appl 15:618–627. https://doi.org/10.1890/03-5342
7. Fu L, Huang T, Wang S, Wang XH, Su LM, Li C, Zhao YH (2017) Toxicity of 13 different antibiotics towards freshwater green algae *Pseudokirchneriella subcapitata* and their modes of action. Chemosphere 168:217–222. https://doi.org/10.1016/j.chemosphere.2016.10.043
8. Nestler H, Groh KJ, Schönenberger R, Behra R, Schirmer K, Eggen RIL, Suter MJF (2012) Multiple-endpoint assay provides a detailed mechanistic view of responses to herbicide exposure in *Chlamydomonas reinhardtii*. Aquat Toxicol 110–111:214–224. https://doi.org/10.1016/j.aquatox.2012.01.014
9. Prado R, Rioboo C, Herrero C, Abalde J, Cid A (2009) Comparison of the sensitivity of different toxicity test endpoints in a microalga exposed to the herbicide paraquat. Environ Int 35:240–247. https://doi.org/10.1016/j.envint.2008.06.012
10. Esperanza M, Cid A, Herrero C, Rioboo C (2015) Acute effects of a prooxidant herbicide on the microalga *Chlamydomonas reinhardtii*: screening cytotoxicity and genotoxicity endpoints. Aquat Toxicol 165:210–221. https://doi.org/10.1016/j.aquatox.2015.06.004
11. Almeida AC, Gomes T, Langford K, Thomas KV, Tollefsen KE (2017) Oxidative stress in the algae *Chlamydomonas reinhardtii* exposed to biocides. Aquat Toxicol 189:50–59. https://doi.org/10.1016/j.aquatox.2017.05.014
12. Chakraborty S, Tiwari B, Singh SS, Srivastava AK, Mishra AK (2017) Differential physiological, oxidative and antioxidative responses of cyanobacterium *Anabaena sphaerica* to attenuate malathion pesticide toxicity. Biocatal Agric Biotechnol 11:56–63. https://doi.org/10.1016/j.bcab.2017.05.011
13. Coquillé N, Ménard D, Rouxel J, Dupraz V, Éon M, Pardon P, Budzinski H, Morin S, Parlanti É, Stachowski-Haberkorn S (2018) The influence of natural dissolved organic matter on herbicide toxicity to marine microalgae is species-dependent. Aquat Toxicol 198:103–117. https://doi.org/10.1016/j.aquatox.2018.02.019
14. Vogs C, Kühnert A, Hug C, Küster E, Altenburger RA (2015) Toxicokinetic study of specifically acting and reactive organic chemicals for the prediction of internal effect concentrations in *Scenedesmus vacuolatus*. Environ Toxicol Chem 34:100–111. https://doi.org/10.1002/etc.2764
15. Vogs C, Altenburger R (2016) Time-dependent effects in algae for chemicals with different adverse outcome pathways: a novel approach. Environ Sci Technol 50:7770–7780. https://doi.org/10.1021/acs.est.6b00529
16. Franz S, Altenburger R, Heilmeier H, Schmitt-Jansen M (2008) What contributes to the sensitivity of microalgae to triclosan? Aquat Toxicol 90:102–108. https://doi.org/10.1016/j.aquatox.2008.08.003
17. Zhang W, Xiong B, Sun WF, An S, Lin KF, Guo MJ, Cui XH (2014) Acute and chronic toxic effects of bisphenol a on *Chlorella pyrenoidosa* and *Scenedesmus obliquus*. Environ Toxicol 29:714–722. https://doi.org/10.1002/tox.21806
18. Hess FD (2000) Light-dependent herbicides: an overview. Weed Sci 48:160-170. https://www.jstor.org/stable/4046249
19. Abdollahi M, Ranjbar A, Shadnia S, Nikfar S, Rezaie A (2004) Pesticides and oxidative stress: a review. Med Sci Monit 6:RA141
20. Aksakal O (2013) Assessment of paraquat genotoxicity on barley (*Hordeum vulgare* L.) seedlings using molecular and biochemical parameters. Acta Physiol Plant 35:2281–2287. https://doi.org/10.1007/s11738-013-1265-2
21. Zhang H, Li J, Ge FP, Zhou JY, Guo KN (2013) Effects of paraquat on the growth of cyanobacteria and green algae. Acta Sci Circum 33(5):1441–1445
22. Strasser RJ, Srivastava A, Govindjee G (1995) Polyphasic chlorophyll a fluorescence transients in plants and cyanobacteria. Photochem Photobiol 61:32–42. https://doi.org/10.1111/j.1751-1097.1995.tb09240.x
23. Samson G, Prášil O, Yaakoubd B (1999) Photochemical and thermal phases of chlorophyll a fluorescence. Photosynthetica 37:163–182. https://doi.org/10.1023/A:1007095619317
24. Strasser BJ, Strasser RJ (1995) Measuring fast fluorescence transients to address environmental questions: the JIP-test. In: Mathis P (ed) Photosynthesis: from light to biosphere. KAP Press, Dordrecht, pp 977–980. https://doi.org/10.1007/978-94-009-0173-5_1142
25. Force L, Critchley C, VanRensen JJS (2003) New fluorescence parameters for monitoring photosynthesis in plants. 1. The effect of illumination on the fluorescence parameters of the JIP-test. Photosynth Res 78:17–33. https://doi.org/10.1023/A:1026012116709
26. Uchiyama M, Mihara M (1978) Determination of malonaldehyde precursor in tissues by thiobarbituric acid test. Anal Chem 86:271–278. https://doi.org/10.1016/0003-2697(78)90342-1
27. Dhindsa RS, Matowe W (1981) Drought tolerance in two mosses: with enzymatic defense against lipid peroxidation. J Exp Bot 32:79–91. https://doi.org/10.1093/jxb/32.1.79
28. Aebi H (1984) Catalase in vitro. Methods Enzymol 105:121–126. https://doi.org/10.1016/S0076-6879(84)05016-3

29. Cheng L, He Y, Tian Y, Liu BY, Zhang YY, Zhou QH, Wu ZB (2017) Comparative biotoxicity of N-Phenyl-1-naphthylamine and N-Phenyl-2-naphthylamine on cyanobacteria *Microcystis aeruginosa*. Chemosphere 176:183–191. https://doi.org/10.1016/j.chemosphere.2017.02.110
30. Roth BL, Poot M, Yue ST, Millard PJ (1997) Bacterial viability and antibiotic susceptibility testing with SYTOX green nucleic acid stain. Appl Environ Microbiol 63:2421–2431
31. Juneau P, Qiu B, Deblois CP (2007) Use of chlorophyll fluorescence as a tool for determination of herbicide toxic effect: review. Toxicol Environ Chem 89:609–625. https://doi.org/10.1080/02772240701561569
32. Schreiber U, Quayle P, Schmidt S, Escher BI, Mueller JF (2007) Methodology and evaluation of a highly sensitive algae toxicity test based on multiwell chlorophyll fluorescence imaging. Biosens Bioelectron 22:2554–2563. https://doi.org/10.1016/j.bios.2006.10.018
33. Kumar KS, Dahms HU, Lee JS, Kim HC, Lee WC, Shin KH (2014) Algal photosynthetic responses to toxic metals and herbicides assessed by chlorophyll a fluorescence. Ecotoxicol Environ Saf 104:51–71. https://doi.org/10.1016/j.ecoenv.2014.01.042
34. Perron MC, Juneau P (2011) Effect of endocrine disrupters on photosystem II energy fluxes of green algae and cyanobacteria. Environ Res 111:520–529. https://doi.org/10.1016/j.envres.2011.02.013
35. Prado R, Garicia R, Rioboo C, Herrero C, Cid A (2015) Suitability of cytotoxicity endpoints and test microalgal species to disclose the toxic effect of common aquatic pollutants. Ecotox Environ Safe 114:117–125. https://doi.org/10.1016/j.ecoenv.2015.01.021
36. Küster A, Pohl K, Altenburger R (2007) A Fluorescence-Based bioassay for aquatic macrophytes and its suitability for effect analysis of non-photosystem II inhibitors. Env Sci Pollut Res 14:377–383. https://doi.org/10.1065/espr2007.04.410
37. Zhan J, Zhu X, Zhou W, Chen H, He C, Wang Q (2016) Thf1 interacts with PS I and stabilizes the PS I complex in *Synechococcus* sp. PCC7942. Mol Microbiol 102:738–751. https://doi.org/10.1111/mmi.13488
38. Nestler H, Groh KJ, Schönenberger R, Eggen RIL, Suter MJF (2012) Linking proteome responses with physiological and biochemical effects in herbicide-exposed *Chlamydomonas reinhardtii*. J Proteome 75:5370–5385. https://doi.org/10.1016/j.jprot.2012.06.017
39. Eullaffroy P, Frankart C, Aziz A, Couderchet M, Blaise C (2009) Energy fluxes and driving forces for photosynthesis in *Lemna minor* exposed to herbicides. Aquat Bot 90:172–178. https://doi.org/10.1016/j.aquabot.2008.09.002
40. Trebst A (2007) Inhibitors in the functional dissection of the photosynthetic electron transport system. Photosynth Res 92:217–224. https://doi.org/10.1007/s11120-007-9213-x
41. Kumar KS, Han T (2010) Physiological response of Lemna species to herbicides and its probable use in toxicity testing. Toxicol Environ Health Sci 2:39–49. https://doi.org/10.1007/BF03216512
42. Jamers A, Coen WD (2010) Effect assessment of the herbicide paraquat on a green alga using differential gene expression and biochemical biomarkers. Environ Toxicol Chem 29:893–901. https://doi.org/10.1002/etc.102
43. Dinis-Oliveira RJ, Duarte JA, Sánchez-Navarro A, Remião F, Bastos ML, Carvalho F (2008) Paraquat poisonings: mechanisms of lung toxicity, clinical features, and treatment. Crit Rev Toxicol 38:13–71. https://doi.org/10.1080/10408440701669959
44. Ananieva EA, Christov KN, Popova LP (2004) Exogenous treatment with salicylic acid leads to increased antioxidant capacity in leaves of barley plants exposed to paraquat. J Plant Physiol 161:319–328. https://doi.org/10.1078/0176-1617-01022
45. Qian HF, Chen W, Sun LW, Jin YX, Liu WP, Fu ZW (2009) Inhibitory effects of paraquat on photosynthesis and the response to oxidative stress in *Chlorella vulgaris*. Ecotoxicology 18:537–543. https://doi.org/10.1007/s10646-009-0311-8
46. Zhang WG, Liu M, Zhang PL, Yu FG, Lu S, Li PF, Zhou JY (2014) Effects of paraquat on photosynthetic pigments, antioxidant enzymes, and gene expression in *Chlorella pyrenoidosa* under mixotrophic compared with autotrophic conditions. Arch Environ Con Toxicol 67:593–600. https://doi.org/10.1007/s00244-014-0067-x
47. Apel K, Hirt H (2004) Reactive oxygen species: metabolism, oxidative stress, and signal transduction. Annu Rev Plant Biol 55:373–399. https://doi.org/10.1146/annurev.arplant.55.031903.141701
48. Foyer CH, Noctor G (2005) Oxidant and antioxidant signalling in plants: a re-evaluation of the concept of oxidative stress in a physiological context. Plant Cell Environ 28:1056–1071. https://doi.org/10.1111/j.1365-3040.2005.01327.x
49. Martinez-Ruiz EB, Martinez-Jeronimo F (2017) Exposure to the herbicide 2,4-D produces different toxic effects in two different phytoplankters: a green microalga (*Ankistrodesmus falcatus*) and a toxigenic cyanobacterium (*Microcystis aeruginosa*). Sci Total Environ 619:1566–1578. https://doi.org/10.1016/j.scitotenv.2017.10.145
50. Yu XB, Hao K, Ling F, Wang GX (2014) Aquatic environmental safety assessment and inhibition mechanism of chemicals for targeting *Microcystis aeruginosa*. Ecotoxicology 23:1638–1647. https://doi.org/10.1007/s10646-014-1303-x
51. Jürgens UJ, Weckesser J (1985) The fine structure and chemical composition of the cell wall and sheath layers of cyanobacteria. Annales de l'Institut Pasteur/Microbiologie. 136(1):41–44. https://doi.org/10.1016/S0769-2609(85)80019-3
52. Atkinson AW, Gunning BES, John PCL (1972) Sporopollenin in the cell wall of *Chlorella* and other algae: ultrastructure, chemistry, and incorporation of (14) C-acetate, studied in synchronous cultures. Planta 107:1–32. https://doi.org/10.1007/BF00398011
53. Allard B, Templier J (2000) Comparison of neutral lipid profile of various trilaminar outer cell wall (TLS)-containing microalgae with emphasis on algaenan occurrence. Phytochemistry 54:369–380. https://doi.org/10.1016/S0031-9422(00)00135-7
54. Scholz MJ, Weiss TL, Jinkerson RE, Jing J, Roth R, Goodenough U, Posewitz MC, Gerken HG (2014) Ultrastructure and composition of the *Nannochloropsis gaditana* cell wall. Eukaryot Cell 13:1450–1464. https://doi.org/10.1128/EC.00183-14
55. Gartner G, Uzunov B, Ingolic E, Kofler W, Gacheva G, Pilarski P, Zagorchev L, Odjakova M, Stoyneva M (2015) Microscopic investigations (LM, TEM and SEM) and identification of *Chlorella* isolate R-06/2 from extreme habitat in Bulgaria with a strong biological activity and resistance to environmental stress factors. Biotechnol Biote Eq 29:536–540. https://doi.org/10.1080/13102818.2015.1013283
56. Xi J, Xu P, Xiang CB (2012) Loss of AtPDR11, a plasma membrane-localized ABC transporter, confers paraquat tolerance in *Arabidopsis thaliana*. Plant J 69:782–791. https://doi.org/10.1111/j.1365-313X.2011.04830.x
57. Fujita M, Fujita Y, Iuchid S, Yamada K, Kobayashid Y, Uranoa K, Kobayashid M, Yamaguchi-Shinozaki K, Shinozaki K (2012) Natural variation in a polyamine transporter determines paraquat tolerance in *Arabidopsis*. Proc Natl Acad Sci 109:6343–6347. https://doi.org/10.1073/pnas.1121406109
58. Fujita M, Shinozaki K (2014) Identification of polyamine transporters in plants: paraquat transport provides crucial clues. Plant Cell Physiol 55:855–861. https://doi.org/10.1093/pcp/pcu032
59. Incharoensakdi A, Jantaro S, Raksajit W, Mäenpää P (2010) Polyamines in cyanobacteria: biosynthesis, transport and abiotic stress response. In: Méndez-Vilas A (ed) Current research, technology and education topics in applied microbiology and microbial biotechnology. Formatex, Badajoz, pp 23–32
60. Theiss C, Bohley P, Bisswanger H, Voigt J (2004) Uptake of polyamines by the unicellular green alga *Chlamydomonas reinhardtii* and their effect

on ornithine decarboxylase activity. J Plant Physiol 161:3–14. https://doi.org/10.1078/0176-1617-00987
61. Drábková M, Matthijs HCP, Admiraal W, Maršálek B (2007) Selective effects of H_2O_2 on cyanobacterial photosynthesis. Photosynthetica 45:363–369. https://doi.org/10.1007/s11099-007-0062-9
62. Esteves SM, Almeida SFP, Gonçalves S, Rimet F, Bouchez A, Figueira E (2018) Sensitive vs. tolerant *Nitzschia palea* (Kützing) W. Smith strains to atrazine: a biochemical perspective. Ecotoxicology 27:860–870. https://doi.org/10.1007/s10646-018-1953-1

Publisher's Note